



Rapidly pulsed reductants for diesel NO_x reduction with lean NO_x traps: Effects of pulsing parameters on performance

Amin Reihani^a, Galen B. Fisher^{b,*}, John W. Hoard^a, Joseph R. Theis^c, James D. Pakko^c, Christine K. Lambert^c

^a Mechanical Engineering Dept., Univ. of Michigan, Ann Arbor, MI 48109, USA

^b Chemical Engineering Dept., Univ. of Michigan, Ann Arbor, MI 48109, USA

^c Ford Motor Company, Dearborn, MI 48124, USA



ARTICLE INFO

Article history:

Received 5 January 2017

Received in revised form 5 July 2017

Accepted 19 July 2017

Available online 23 July 2017

Keywords:

Lean NO_x traps

Rapid HC pulsing

High temperature NO_x reduction

Fuel penalty

N₂O/NH₃ selectivity

ABSTRACT

The use of Rapidly Pulsed Reductants (RPR) provides a method for injecting hydrocarbons in rapid pulses ahead of a lean NO_x trap (LNT) with the goal of achieving greater than 90% NO_x conversion at temperatures as high as 600 °C. This approach was recently discussed under the name Di-Air by Toyota. It may be useful for diesel vehicles with smaller engines that cannot conveniently accommodate urea SCR technology. A further goal of RPR is to reduce the fuel penalty associated with the fuel injections used to purge the LNT.

The focus of this study was on understanding this approach in the exhaust temperature range of 450 °C to 600 °C. The impact of pulsing parameters, i.e., pulse frequency, pulse amplitude, and duty cycle (i.e., ratio of pulse-on/total-cycle-time) on RPR performance was investigated using ethylene injection into simulated exhaust with a research LNT catalyst over a wide range of conditions. A novel injection system was designed that allowed for the investigation of previously unexplored areas of high frequency (up to $f = 100$ Hz) and produced pulse durations as short as a millisecond. NO_x storage capability was found to be essential for RPR operation. An optimal pulsing frequency was always found for a given set of flow conditions that produced a maximum NO_x conversion while holding the fuel penalty (i.e., hydrocarbon dose) constant. The optimal pulsing frequency, usually on the order of 1 Hz, was dependent on a number of parameters including the flow velocity, concentration of injected hydrocarbons, and operating temperature. The effects of pulse duty cycle and amplitude, which together determine the amount of injected reductant or the fuel penalty, were investigated separately. Regardless of pulsing frequency and duty cycle, pulses of injected hydrocarbon large enough in magnitude to generate a rich mixture were necessary during the pulse in order to achieve high NO_x conversion. Lean or even stoichiometric pulses did not achieve significant NO_x conversion. However, even with the rich pulses, the cycle-averaged air/fuel ratio remained net lean in this work.

In the main temperature range of this study (450–600 °C), where the NO_x storage capacity of the LNT was very limited, RPR operation could be divided into two frequency regimes, one below and one above the optimum frequency. At injection frequencies below the optimum frequency, it was observed that the NO_x conversion improved as the frequency increased. This was primarily because the duration of the lean period was decreasing, increasing the average NO_x storage efficiency during the lean period while still maintaining sufficient durations of the rich period to adequately purge the LNT. At injection frequencies above the optimum frequency, reductant mixing and its parasitic consumption by the gas phase O₂ resulted in inadequate purging of the LNT, causing the NO_x conversion to drop from the maximum value. These competing factors led to the maximum NO_x conversion observed during RPR operation for a LNT at temperatures as high as 600 °C for a specified fuel penalty.

© 2017 Elsevier B.V. All rights reserved.

1. Introduction

Increasingly stringent regulations on greenhouse gases and new standards on fuel economy for vehicles encourage the use of lean burn gasoline and diesel engines for their inherently higher fuel conversion efficiency [1,2]. However, due to the lean exhaust envi-

* Corresponding author.

E-mail address: gbfisher@umich.edu (G.B. Fisher).

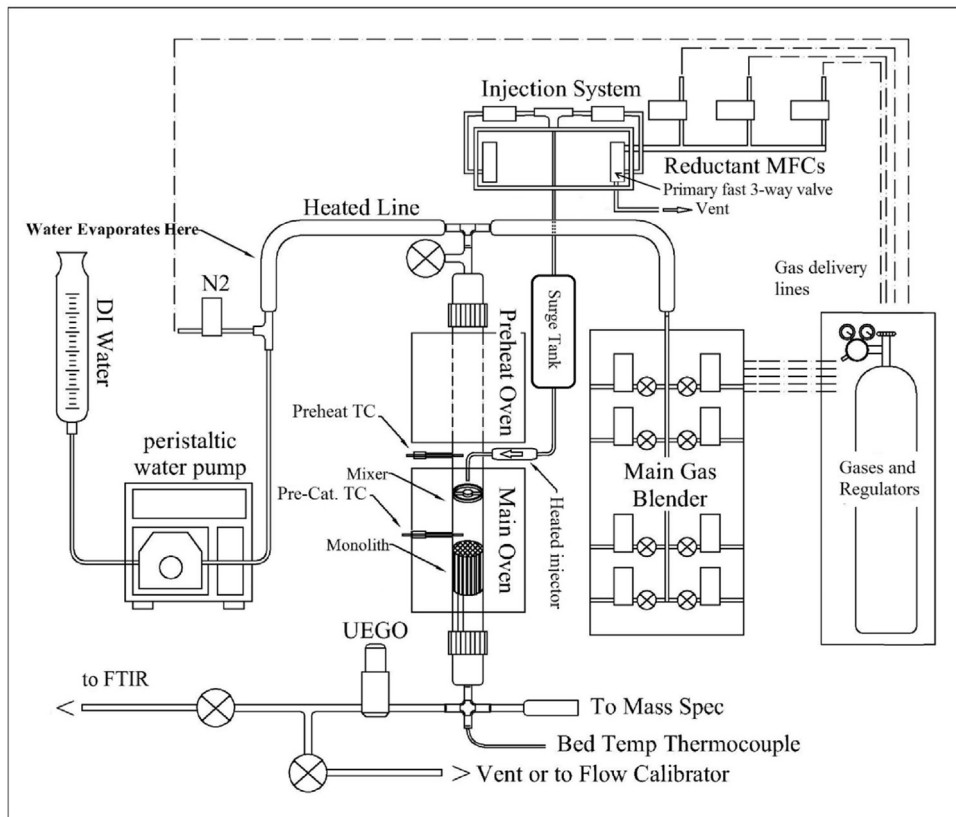


Fig. 1. Schematic of bench reactor.

ronment, diesel NOx emission control is challenging, especially with recent, more stringent legislation such as the US Tier 3 and European Real-Driving Emission (RDE) regulations. Current diesel NOx aftertreatment methods such as urea SCR and lean NOx traps (LNTs) are expected to require modifications or improvements in order to satisfy these regulations. For example, vehicles equipped with SCR are expected to have a 50% increase in urea consumption from current Euro 6 vehicles to meet future RDE requirements [3].

LNTs are currently employed on light duty diesel vehicles with smaller engines (typical displacement ≤ 2.0 L) [4,5]. Numerous studies have been performed to assess the effects of pulsing parameters and hydrocarbon type on the performance of LNT catalysts. Li et al. [6] found that the overall NOx conversion under cyclic lean/rich conditions was dependent on the balance of lean/rich timing. The NOx conversion at moderate temperatures of 250–400 °C was found to be a direct function of reaction stoichiometry. That is, the quantity of trapped NOx under lean conditions was balanced by the quantity of reductants during the rich step. On the other hand, the NOx conversion was limited by reaction kinetics at lower temperatures and by the decreasing NOx storage capacity of the LNT at high temperatures [6].

In terms of reductant type, CO has been found to be an effective reductant over the entire temperature range, while hydrocarbons were found to be more effective at higher temperatures. H₂ is an effective reductant primarily at lower temperatures because of the non-selective consumption of H₂ in the system as the temperature increases [7–10]. As far as reaction products are concerned, ammonia is formed during regenerations with H₂. In addition, using *in situ* FTIR, Ba and Al isocyanates have been observed on Pt–Rh/Ba/Al₂O₃ catalysts during regeneration with CO as a result of spillover from the precious metal sites; the hydrolysis of these isocyanates has been proposed as the pathway to NH₃ formation when CO was the reductant [11]. At low temperatures (e.g., 250 °C),

the usual inhibiting effect of CO was observed with operando IR spectroscopy. The presence of stable nitrosyl species lasting up to 60 s was also observed at this temperature, which caused the preferential production of N₂O for shorter total periods and insufficient reduction of the N₂O for longer total periods because NO inhibits the re-adsorption of the N₂O [7].

Previous studies using conventional LNTs have shown the negative effect of feedgas CO₂ on NOx conversion due to the competition of NOx and CO₂ for the storage sites [12]. Overall, a major drawback of conventional LNT technology is the limited operating temperature window for high NOx conversion, typically 200–450 °C, although this window can be influenced by the LNT formulation [4,13,14]. Some of the ceria-containing LNTs used on diesels can store NOx at lower temperatures (~150 °C), but they are less effective at higher temperatures [15,16]. At high engine loads the post-turbo exhaust temperature can exceed 600 °C, and gas hourly space velocities (GHSV) can reach 150,000 h⁻¹. Under these conditions, the NOx conversion of conventional LNTs drops significantly. Therefore, in high load driving cycles, the use of urea SCR is preferred if packaging space is available and it can reduce emissions by as much as 30% compared to a LNT [3]. However, for applications where it would be difficult to install a urea tank and injection system due to space constraints and/or cost considerations, it would be desirable to expand the operating window of the current LNT system to higher temperatures and flow rates. Toyota reported that a system called Di-Air can provide improved NOx conversion at temperatures as high as 600 °C and at higher flow rates [17,18]. This system uses frequent injections of hydrocarbons ahead of a conventional LNT catalyst. We have assessed this system under the name Rapidly Pulsed Reductants (RPR).

Prior work was performed to elucidate the underlying mechanism of Di-Air, and some of these studies led to the conclusion that adsorbed NOx “intermediates” generated on the catalyst surface

Table 1

Species concentrations during rich/lean periods (i.e., injection on/off) for a range of λ_{pulse} values used in this study during a 15% duty cycle pulse.

| | Lean | Rich (during pulse) | | | | | | |
|-----------------------------------|------|---------------------|------|------|------|------|------|------|
| | | 0.90 | 0.85 | 0.80 | 0.75 | 0.7 | 0.65 | 0.6 |
| Lambda | 1.18 | 0.90 | 0.85 | 0.80 | 0.75 | 0.7 | 0.65 | 0.6 |
| Ar or N ₂ (%) | 84.2 | 84.8 | 84.9 | 85.0 | 85.2 | 85.4 | 85.5 | 85.7 |
| O ₂ (%) | 2.0 | 1.8 | 1.7 | 1.7 | 1.6 | 1.6 | 1.5 | 1.5 |
| CO ₂ (%) | 9.2 | 8.2 | 8.0 | 7.8 | 7.6 | 7.3 | 7.0 | 6.7 |
| NO (ppm) | 300 | 269 | 262 | 254 | 246 | 238 | 229 | 219 |
| H ₂ O (%) | 4.6 | 4.1 | 4.0 | 3.9 | 3.8 | 3.7 | 3.5 | 3.4 |
| C ₂ H ₄ (%) | 0.00 | 1.04 | 1.28 | 1.52 | 1.79 | 2.06 | 2.36 | 2.68 |

together with partially oxidized hydrocarbons resulting from the rapidly pulsed reductants are responsible for the high NO_x conversion of Di-Air [18,19]. It was observed that intermediates generated from HCs, such as R-NCO and R-CN, have a larger adsorption energy than the intermediates generated from CO or bulk nitrates and can adsorb onto the surface for a number of seconds at temperatures as high as 600 °C [19]. However, it is not clear whether all of these intermediates contribute to the NO_x conversion with Di-Air. It should be mentioned that Bisajji et al. claimed that the flow remained lean during the hydrocarbon injections, and high NO_x conversion activity was achieved at high temperatures by the formation of stable intermediates such as R-NCO which converted to N₂ during the periods between injections [19]. However, under our test conditions, a net rich exhaust mixture was necessary during the hydrocarbon injections in order to achieve significant NO_x conversion at temperatures above 450 °C. Similar findings have been reported by other researchers [12], who also suggested that the limited NO_x storage capacity of the LNT above 400 °C and the decomposition of Ba(NO₃)₂ were not the limiting factors in the reaction. Instead, it was proposed that the stability of HC intermediates on the surface was the limiting factor for the reaction at temperatures near 600 °C. However, in our work, the limited NO_x storage capacity of the LNT at high temperatures was found to have a major influence on the RPR process.

In this study, the effects of pulsing frequency ($f = 1/P$, where P is the total rich/lean cycle period), amplitude (in terms of air-fuel equivalence ratio or λ_{pulse}), and duty cycle (defined as: rich duration/total cycle period) on RPR performance were investigated at temperatures above 450 °C. Pulses of reductants were injected into the main flow of the simulated exhaust gas upstream of a mixer and a conventional LNT catalyst on a synthetic flow reactor. The hydrocarbon injection system utilized high speed fuel injectors and miniature solenoid valves designed to inject pulses as rapidly as 100 Hz. Also, the data obtained from the aforementioned parameter space provided insight into the underlying RPR mechanism and helped to suggest a theoretical model to elucidate the observations at temperatures above 450 °C. This work led to the discovery of optimal pulsing parameters as a function of operating conditions (i.e., flow rate, temperature, and species concentrations) that generated the maximum NO_x conversion while minimizing the fuel penalty associated with the hydrocarbon injections.

2. Experimental setup

The experimental setup consisted of a synthetic flow reactor, supply gases, injection system, control and data acquisition unit, interface computer, and measurement instrumentation. Fig. 1 depicts a schematic of the flow reactor and the quartz tube used for the catalyst sample. The reactor included a number of mass flow controllers (MFCs) and a water evaporator unit for the main flow

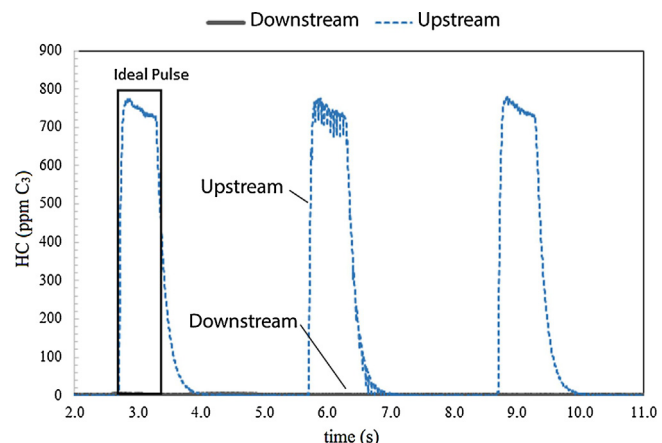


Fig. 2. Pulsing of propane measured by fast-FID with a 200 Hz sampling rate. Upstream curve measured at inlet face of an oxidation catalyst. Downstream curve measured downstream of catalyst.

composition and three additional MFCs for injecting the reductants. The main flow was a specified composition of H₂O, CO₂, NO, NO₂, and O₂, while the reductant was typically C₂H₄. Either N₂ or Ar was used as the carrier gas. It was found that the choice of carrier gas had no effect on the NO_x conversion results. However, the choice of Ar is preferred since it allows for measurement of N₂ in the mass spectrometer and a closure of the nitrogen balance in the measurements. Using the data obtained from FTIR, a balance for carbon was obtained in the experiments. However, obtaining a balance for hydrogen was not possible due to the existence of considerable concentrations of water which caused interference in the mass spectrometer. The nominal species concentrations as well as the lambda values during the lean (main flow) and rich (pulsing) periods at different λ_{pulse} values are shown in Table 1. As can be seen in Fig. 1, the test rig consisted of a main flow path to carry the simulated exhaust gases, the mixer, and the injection tube which was connected to the pneumatic injection system.

The following are the components of the injection system with upstream to downstream order on the injection flow path. (a) A mass flow controller for gas phase reductants (or carrier gas in case of liquid reductants) that is always flowing at the desired injection flow, (b) a primary 3-way miniature valve with a 6 ms switching time that is either venting to atmospheric pressure or directing the flow towards the injection path, (c) a pressurized surge tank with a volume of 1L which is used to dampen high frequency pressure oscillations from the primary valve and maintain positive pressure for the secondary valve, (d) a liquid hydrocarbon evaporator unit, which is only used in the case of liquid hydrocarbons, (e) a secondary heated fast valve. A Bosch NG12 natural gas port fuel injector was used for this purpose, (f) Injection nozzle inside the reactor tube. The mixer and injection system were designed with the aim of achieving high frequency pulses with good radial mixing of the injected reductants while simultaneously minimizing the mixing in the axial direction. This mixing pattern was found to be of critical importance for high RPR performance. A Cambustion HFR500 Fast Flame Ionization Detector (fast FID) was used to experimentally measure and tune the mixing and injection circuit with a different setup of the flow reactor. A sample pulse with the optimized mixer is shown in Fig. 2, which indicated a near “plug-flow” pulse upstream of an oxidation catalyst and essentially zero breakthrough of C₃H₈ downstream of the oxidation catalyst when operated with a stoichiometric amount of O₂ and C₃H₈, indicating uniform radial mixing [10].

The measurement system consisted of a MKS FTIR Multigas 2030 analyzer and a MKS Cirrus 2 mass spectrometer. Also, a wide band

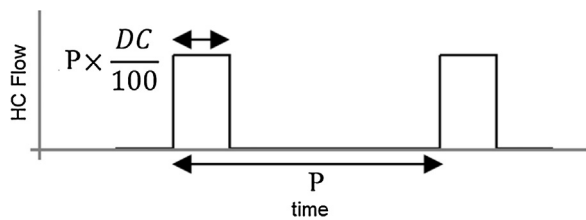


Fig. 3. Schematic of total rich/lean cycle period, P (s), and duty cycle, DC (%).

lambda sensor (Bosch LSU 4.2) was installed at the outlet of the reactor to monitor the stoichiometric ratio of the system. It was also used as a diagnostic tool to detect the failure of the system to maintain the desired air/fuel ratio. For each experiment, the main flow concentrations were first recorded during bypass operation and averaged for a sufficient time to ensure a steady response from the MFCs and a stable flow temperature. After directing the exhaust through the sample, the time response of the system in a specified test condition was recorded at the outlet of the reactor with a 1 Hz sampling frequency along with the inlet and catalyst bed temperatures, MFC feedback, and lambda sensor output until stabilized operation was achieved. The 1 Hz sampling frequency was not sufficient to detect individual pulses at the higher injection frequencies; therefore, this sampling frequency was used to determine the cycle averaged concentrations of the various gas species at the reactor outlet. Data acquisition and control of the system was performed using a NI cDAQ chassis and I/O modules. Specific care was taken in the design of the electronics and control circuitry for the reductant injection system solenoid valves and injectors in order to decrease the response time of the system and enable higher pulsing frequencies. Finally, a LabVIEW (National Instruments) program was developed to set the control inputs for the system and record the experimental data.

The LNT sample used in this study was a research Pt/Rh LNT formulation with 3.18 g/L (90 g per cubic foot (gpcf)) of precious metal (Pt/Pd/Rh = 8/0/1) on a 400 cpsi (62 cell/cm²) cordierite monolith with a 6.5 mil (165 µm) wall thickness, 25 mm length, and 19 mm in diameter. The washcoat contained barium, a proprietary high temperature NO_x storage component, and no ceria. The sample was degreened with 10% oxygen at 700 °C for two hours. For comparison with the LNT, a three-way catalyst (TWC) containing 2.83 g/L (80 gpcf) of precious metal (Pt/Pd/Rh = 0/78/2), oxygen storage materials, and no NO_x storage components was degreened in the same manner as the LNT sample and tested.

One of the primary goals of this study was to investigate the dependence of the optimal frequency on various operating conditions, such as the temperature, space velocity (SV), and gas phase concentrations. In the frequency sweep tests, pulses with $\lambda_{pulse} = 0.83$ were used. Based on main flow composition (Table 1) the time averaged flow with a duty cycle of 15% was net lean with $\lambda_{ave} = 1.10$. The pulsing frequency was varied between $f = 20$ Hz to 0.0167 Hz (i.e., $P = 0.05$ s to 60 s), thus covering a broad range of pulsing frequencies, where low-frequency pulses ($f = 0.01$ – 0.02) are similar to those used in conventional LNT applications. Please note that, generating a pulse with a frequency higher than ~ 5 Hz which possesses the desired radial and axial mixing uniformities for RPR process is very difficult both on real engine applications and a flow reactor scale. Although not practical, data with pulsing frequencies up to 20 Hz are presented in this study, to explore the behavior of the RPR process in that very high frequency regime. The inlet temperature was held at 600 °C except for the temperature sweep experiments where the inlet temperature was varied from 150 °C to 650 °C. Space velocities (SV) of approximately 30,000 h⁻¹, 40,000 h⁻¹ and 50,000 h⁻¹ were used, based on geometric catalyst volume and flow measured at 20 °C. A moderately active hydrocar-

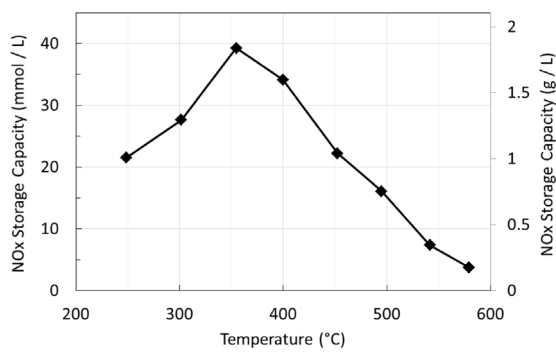


Fig. 4. Effective NO_x storage capacity of the LNT sample as a function of catalyst temperature.

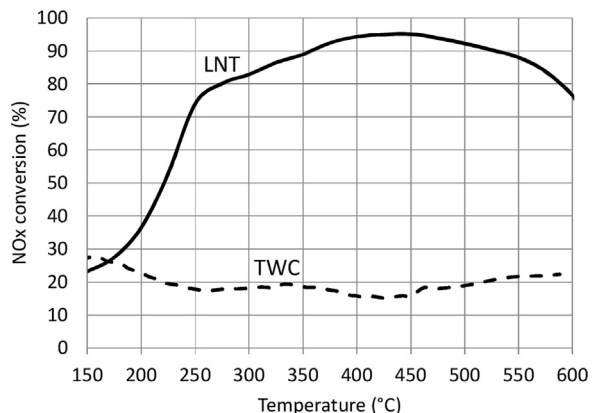


Fig. 5. NO_x conversion measured for RPR experiment with ethylene ($f = 0.33$ Hz, $\lambda_{pulse} = 0.76$, $SV = 30,000$ h⁻¹) on a LNT catalyst and a three-way catalyst (TWC) without NO_x storage materials under similar conditions ($f = 0.33$ Hz, $\lambda_{pulse} = 0.78$, $SV = 30,000$ h⁻¹).

bon (ethylene) was chosen as the main reductant. The pulse duty cycle (as defined in Fig. 3) was varied from 5% to 30%.

3. Results

3.1. NO_x storage capacity

The effective NO_x storage capacity of the LNT sample as a function of catalyst temperature is shown in Fig. 4. At each temperature, the NO_x storage capacity (NSC) was measured by a 5 min cycle of reduction (1.8% CO, 0.3 H₂, 10% CO₂, 5% H₂O) followed by a 10 min NO_x storage cycle under lean conditions (5% O₂, 10% CO₂, 5% H₂O, 670 ppm NO) to achieve a complete saturation of the surface with adsorbed NO_x. The stored NO_x was computed by integrating the difference in inlet and outlet NO_x fluxes over the storage cycle. A maximum NO_x capacity of approximately 40 mmol/L of catalyst was found at 350 °C, while at 600 °C the capacity dropped to less than 3.75 mmol/L of catalyst. In terms of mass, the peak capacity was 1.84 g NO₂/L of catalyst, dropping to less than 0.18 g NO₂/L of catalyst at 600 °C.

3.2. Necessity of NO_x storage material

RPR experiments were performed on both the LNT and the TWC with $f = 0.33$ (P = 3 s), duty cycle = 15%, and a λ_{pulse} of 0.78. Fig. 5 shows that the Pd/Rh TWC with oxygen storage but no NO_x storage components provided much lower NO_x conversion than the LNT over the entire temperature range. In fact, the NO_x conversion of the TWC was only slightly better than the percentage of rich time for a 15% duty cycle, suggesting that the TWC provided NO_x conversion

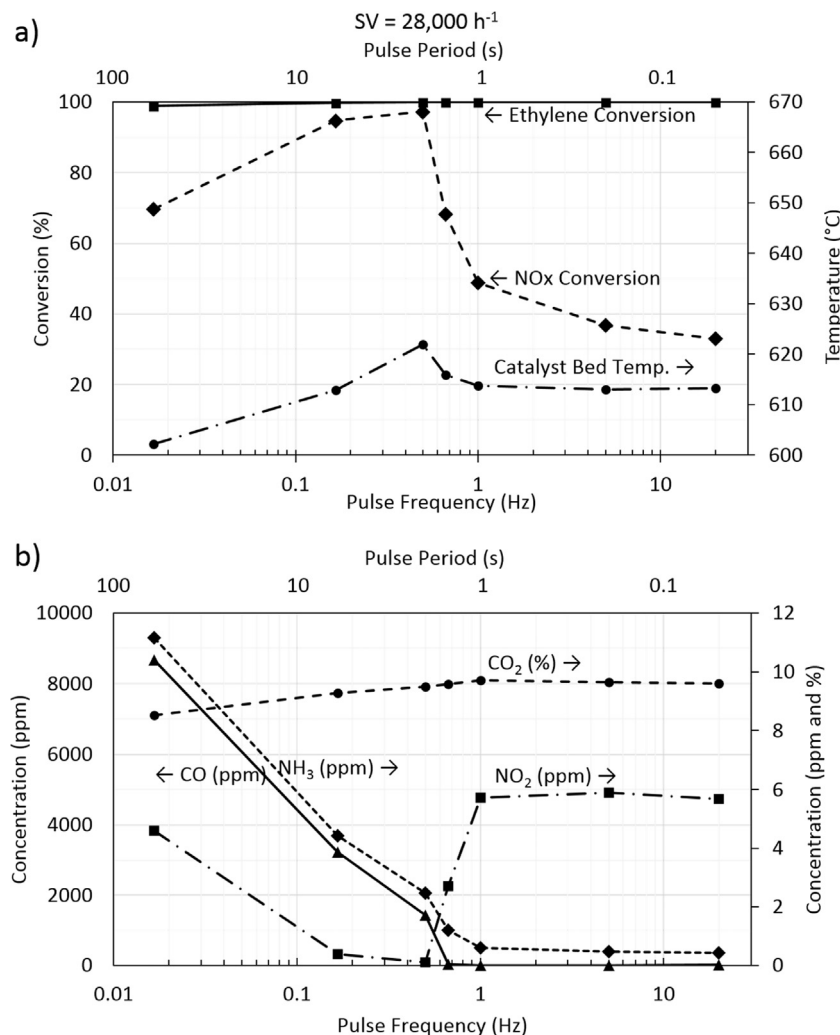


Fig. 6. RPR frequency sweep results at 600 °C inlet temperature, 15% duty cycle, $\lambda_{\text{pulse}} = 0.83$, and $SV = 28,000 \text{ h}^{-1}$.

only during the rich period and very little NO_x conversion during the lean period. These results indicated that NO_x storage capability was needed for the RPR process to work, even though the amount of NO_x stored on the LNT at high temperatures was low. In addition, another factor in the difference between the NO_x conversion over a TWC and a LNT may be the absence of Pt on this TWC which is an active NO_x oxidation catalyst.

3.3. Space velocity and frequency

Figs. 6–8 show the effects of frequency variation at space velocities of 28,000, 40,000, and 51,800 h^{-1} , respectively. The duty cycle was 15%, and Table 1 shows the species concentrations and λ values for both lean and rich periods. Fig. 6(a) shows the NO_x conversion, ethylene conversion, and cycle averaged catalyst bed temperature for a space velocity of 28,000 h^{-1} as a function of pulse frequency in the bottom horizontal axis (for convenience pulse period, P, is included in the top horizontal axis) in a semi-logarithmic format. The existence of a maximum in NO_x conversion in the frequency domain has not been reported previously, and indicates the existence of an optimal pulsing frequency to achieve the highest NO_x conversion for a constant fuel penalty and a defined set of operating conditions. The ethylene conversion was very high (>98.9%) throughout the entire frequency range. It approached 100% at higher pulsing frequencies and decreased slightly as the frequency was decreased (i.e., increasing duration of hydrocarbon injections).

Since there is insufficient O₂ during the purges to consume all of the ethylene, this high conversion can be partly attributed to effective steam reforming of the ethylene by the catalyst. However, this could be less typical for small alkanes such as ethane or propane [20,21].

We also see in Fig. 6(a) that the time averaged bed temperature initially increased as the pulsing frequency was increased from conventional LNT mode to RPR mode, and the bed temperature reached a maximum at the frequency providing the highest NO_x conversion. The bed temperature then decreased slightly as the frequency continued to increase beyond the optimal value. Fig. 6(b) shows the concentrations of CO, CO₂, NO₂, and NH₃ during the same experiment as a function of pulsing frequency. The CO concentration decreased while the CO₂ concentration increased as the pulsing frequency increased, indicating a more complete oxidation of injected ethylene to CO₂ and H₂O at the higher frequencies. The CO concentration was less than 10 ppm for pulsing frequencies above the optimal frequency, which indicated good axial mixing of the reductants with the main flow and more complete oxidation of the reductants. In Fig. 6(b), the cycle averaged NH₃ concentrations were low at all frequencies at 600 °C. The NH₃ concentration decreased as the pulsing frequency increased; this trend was also observed previously during Di-Air operation [12]. The NH₃ concentration asymptotically approached zero around the optimal frequency and remained there at higher frequencies.

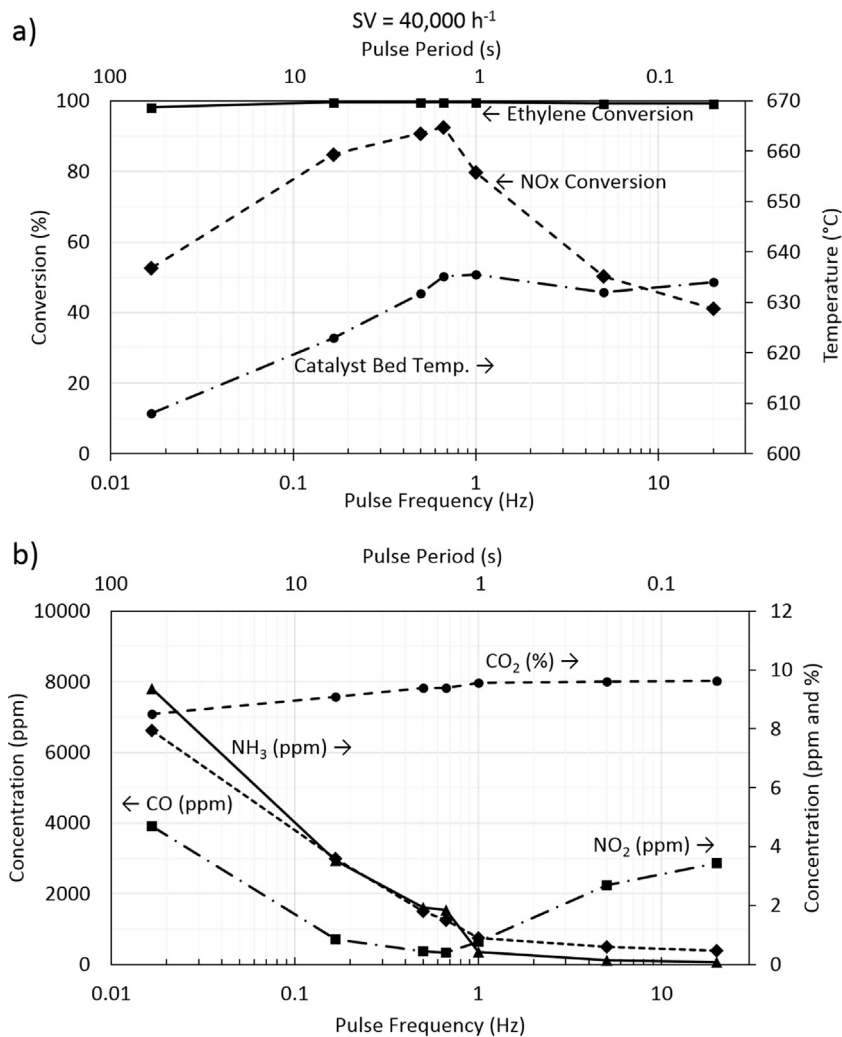


Fig. 7. RPR frequency sweep results at 600 °C inlet temperature, 15% duty cycle, $\lambda_{\text{pulse}} = 0.83$, and $SV = 40,000 \text{ h}^{-1}$.

Figs. 7 and 8 show results similar to those in Fig. 6 for space velocities of 40,000 h⁻¹ and 51,800 h⁻¹, respectively. As seen in Fig. 7(a), the NOx conversion curve displayed a similar shape to Fig. 6, except that the optimal frequency of 0.67 Hz at $SV = 40,000 \text{ h}^{-1}$ was slightly higher than the optimum value of 0.5 Hz at $SV = 28,000 \text{ h}^{-1}$. The exotherm of the reaction in Fig. 7 shows the same trend as in Fig. 6; however, the maximum catalyst bed temperature increased by $\Delta T = 35^\circ\text{C}$ from the inlet compared to the maximum increase of 22°C at 28,000 h⁻¹. Since the flow composition remained constant for all space velocities, the adiabatic temperature rise should have remained the same. However, the ratio of the heat losses to the total exothermic heat decreased as the flow rate increased, resulting in the higher measured bed temperature increase. Fig. 8 shows the results of the frequency sweep at $SV = 51,800 \text{ h}^{-1}$ which indicated that the maximum in the NOx conversion was at $f = 0.71 \text{ Hz}$, which again was shifted slightly toward higher frequencies. In addition, a slight reduction in ethylene conversion was observed at these high flow rates, especially at the lower pulsing frequencies. In contrast with the near zero levels of CO at the optimal frequency at the lower space velocities, Fig. 8(b) shows that there was a considerable CO concentration at and above the optimal frequency for $SV = 51,800 \text{ h}^{-1}$. In addition, a maximum catalyst bed temperature increase of $\Delta T = 63^\circ\text{C}$ from the inlet was observed for $SV = 51,800 \text{ h}^{-1}$, which was higher than the maximum increase of 35°C at 40,000 h⁻¹. From the frequency sweep tests, it was concluded that there exists an optimal pulsing frequency at

each SV to achieve the maximum NOx conversion for a constant fuel penalty. Figs. 6–8 display the NOx conversion vs. frequency curves for the different space velocities and demonstrate that the peak in NOx conversion decreased and the optimal frequency increased as the space velocity increased.

To obtain more direct evidence of the axial mixing of reductants that could account for the drop in NOx conversion at high frequencies, an experiment was conducted to measure the axial distribution of hydrocarbon (HC) pulses entering the catalyst. A measurement of total HC concentration was performed using a Cambustion HFR500 fast-FID probe at the inlet of the catalyst. A sampling frequency of 250 Hz was used, with a low pass Butterworth filter with 55 Hz cutoff frequency to eliminate the measurement noise caused by the AC power. These experiments were performed with propylene at pulsing frequencies ranging from 1/6 Hz to 20 Hz with Ar as the carrier gas to eliminate any gas phase oxidation of the pulse. Fig. 9 depicts the measured HC pulse concentration normalized by the ideal plug flow pulse concentration (shown as blue lines) as a function of time at different pulsing frequencies for a SV of 28,000 h⁻¹ and an inlet temperature of 600 °C. As can be seen, a larger portion of the pulse was axially mixed and a smaller portion of the pulse remained rich as the pulsing frequency was increased. At the highest frequency, the pulses were almost completely mixed, and the fast-FID measurements showed nearly steady state lean conditions.

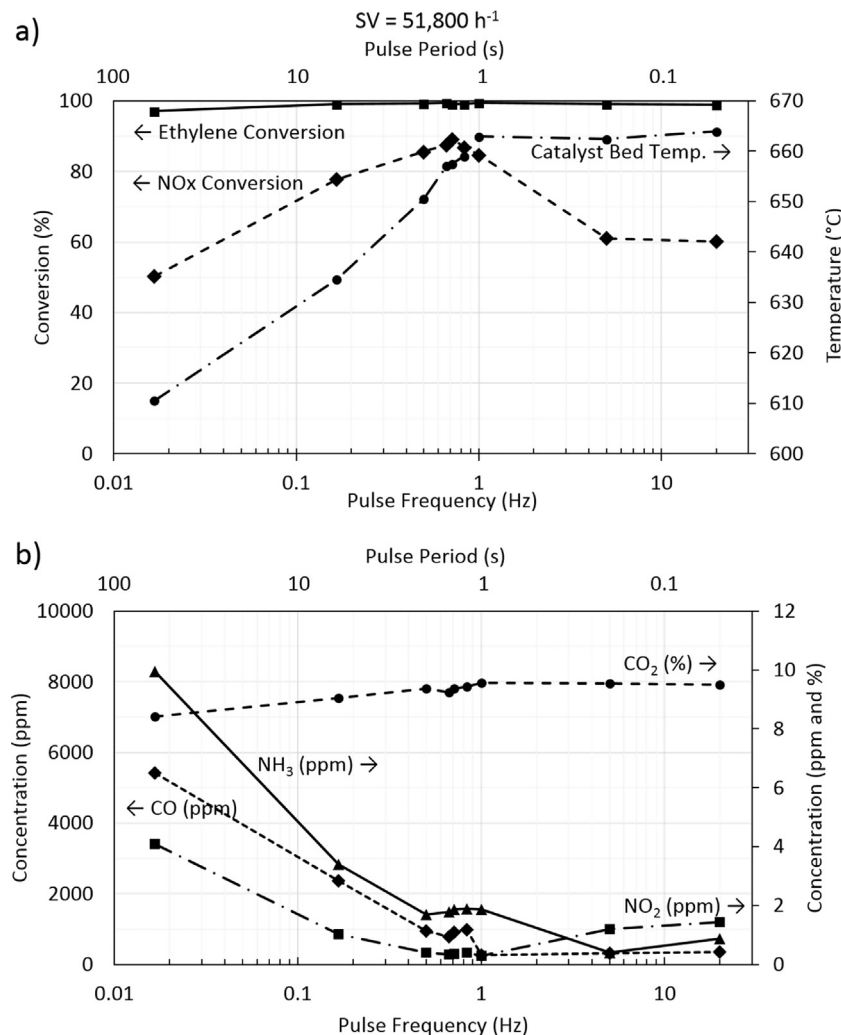


Fig. 8. RPR frequency sweep results at 600 °C inlet temperature, 15% duty cycle, $\lambda_{\text{pulse}} = 0.83$, and $SV = 51,800 \text{ h}^{-1}$.

3.4. Pulse amplitude (λ_{pulse})

An important metric in LNT (and RPR) operation is the fuel penalty associated with reductant pulses, which scales with pulse amplitude and duty cycle. Fig. 10 illustrates the calculated ratio of fuel penalty/duty cycle pulse as a function of pulse amplitude (in terms of λ_{pulse}) for different main flow lean λ values. Therefore, the fuel penalty in each case is equal to the vertical axis value multiplied by the duty cycle. The fuel penalty is calculated by assuming complete combustion products in the exhaust flow with 10% CO_2 and 10% H_2O which is close to diesel engine exhaust concentrations in terms of carbon and hydrogen content. As can be seen, the fuel penalty increases to very high values as the exhaust becomes leaner. Therefore, on real engine applications, it is preferred to use RPR only under high load conditions where the exhaust is closer to stoichiometric conditions ($\lambda < \sim 1.3$).

The effect of increasing the rich magnitude of the pulses by increasing the reductant concentration was investigated by sweeping the λ_{pulse} from 0.63 to 0.93 for pulsing frequencies of 0.05–2 Hz while maintaining the duty cycle at 15%, the inlet temperature at 600 °C, and the SV at 30,000 h⁻¹. The curves of Fig. 11 show the NOx conversion as a function of the micromoles of delivered reductant per pulse for seven different pulsing frequencies. The solid lines represent the data at a constant frequency (i.e., isofrequency curves). Since the duty cycle of the pulses remained constant, the average reductant flow and hence the fuel penalty was constant

for points with the same rich λ_{pulse} , and these are shown as dotted isofuel penalty curves. The maximum NOx conversion as a function of pulsing frequency was evident for λ_{pulse} of 0.8–0.73; however, it was not observed for $\lambda_{\text{pulse}} = 0.63$ since the optimal frequency apparently occurred at higher frequencies than those tested. The optimal pulsing frequency was dependent on λ_{pulse} , and the general trend was that it increased as the pulses became richer. Also, the NOx conversion improved as the pulses became richer at a given pulsing frequency. However, as the pulses became richer than $\lambda_{\text{pulse}} = 0.8$ to 0.75, the slope of the isofrequency curves decreased (e.g., compare the slope at points A and B), indicating that there was diminishing improvement in NOx conversion (per micromole of HC) as the pulses became richer than ca. $\lambda_{\text{pulse}} = 0.75$. For a given fuel penalty, these curves allow one to choose the frequency that provides the highest NOx conversion for a given set of operating conditions (e.g., flow velocity, reductant concentration, and temperature). It was mentioned earlier that, regardless of the pulsing frequency, the NOx conversion was very low at 600 °C with lean or stoichiometric pulses, and rich pulses were required to obtain significant NOx conversion, although the time-averaged flow remained net lean. In addition, Fig. 11 shows that the NOx conversions were relatively low even when the λ_{pulse} was 0.92, suggesting that the λ_{pulse} must achieve a certain minimum level (e.g., 0.80–0.85) in order to adequately purge the LNT and obtain high NOx conversions.

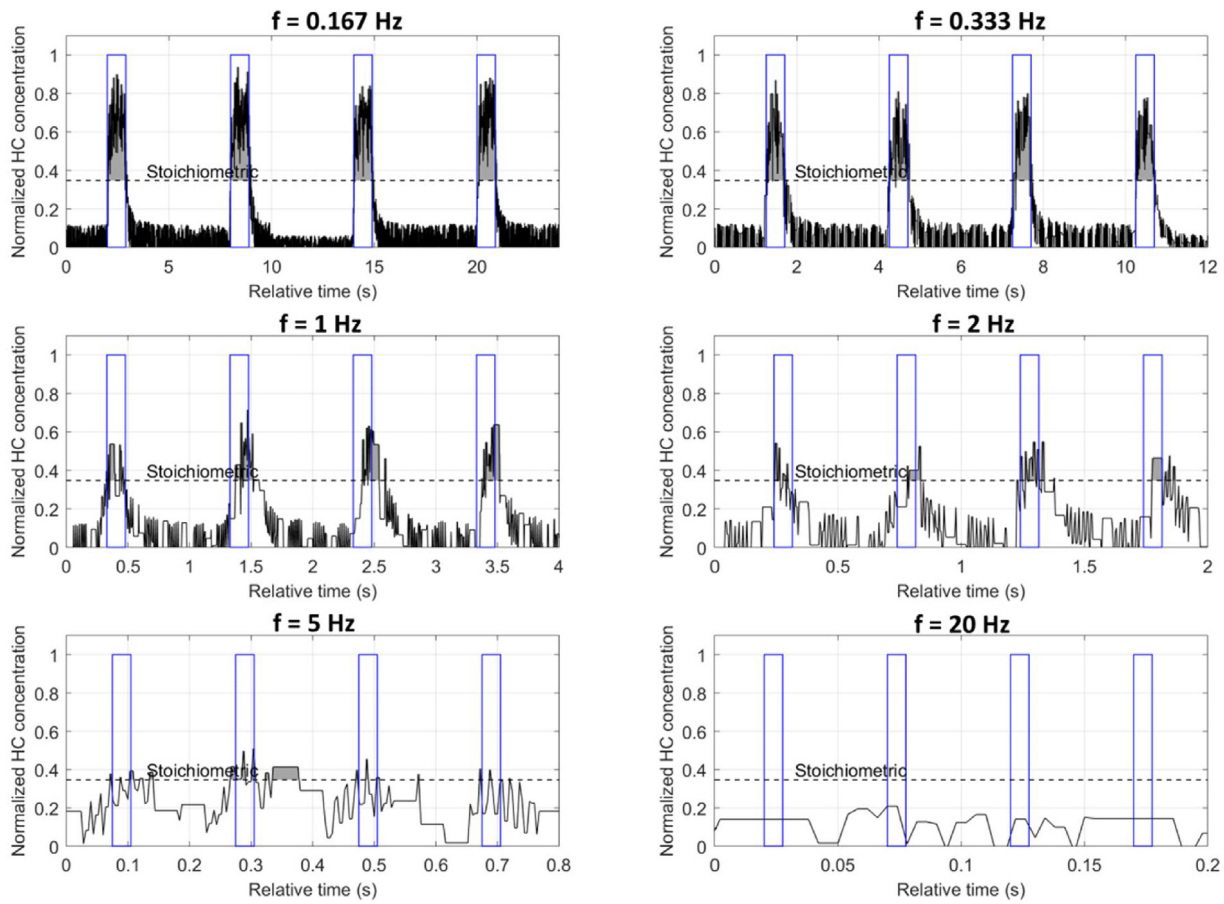


Fig. 9. Propylene pulsed in Ar flow at inlet $T = 600^\circ\text{C}$, 15% duty cycle, $\text{SV} = 28,000 \text{ h}^{-1}$ and frequencies = 0.167, 0.333, 1, 2, 5, and 20 Hz. Black line shows temporal distribution of HC (propylene) concentration, normalized based on the concentration of perfect plug flow pulses (blue lines) at catalyst inlet. Dashed line shows stoichiometric propylene level. Grayed area shows fraction of pulse that is rich. (For interpretation of the references to colour in this figure legend, the reader is referred to the web version of this article.)

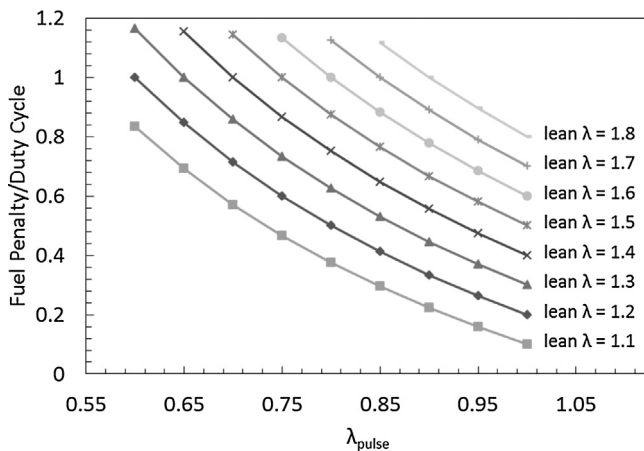


Fig. 10. The ratio of fuel penalty/duty cycle pulse as a function of λ_{pulse} for different overall main flow lean λ values. The fuel penalty is calculated by assuming complete combustion products in an exhaust flow with 10% CO_2 and 10% H_2O .

3.5. NO_x concentration

To gain insight into the underlying mechanism and rate limiting steps important for RPR performance, the effect of the NO_x concentration on the optimal pulsing frequency was assessed. Except for the higher NO_x concentration, the test conditions were the same as for the low NO_x concentration. For space velocities of $28,000 \text{ h}^{-1}$, $40,000 \text{ h}^{-1}$, and $51,000 \text{ h}^{-1}$, Fig. 12(a), (b), and (c) show that the

change in NO concentration from the baseline value of 300 ppm to 810 ppm had no effect on the optimal pulsing frequency. However, the NO_x conversion dropped over the entire frequency range as the NO_x concentration increased. For example, at the space velocity of $40,000 \text{ h}^{-1}$, the maximum NO_x conversions dropped from 92% to 79% as the NO_x concentration increased from 300 to 810 ppm. The ethylene conversion also dropped slightly as the NO_x concentration increased. In addition, the N_2O and NH_3 selectivities (data not shown) were slightly increased for the 810 ppm feedgas NO_x concentration.

3.6. Catalyst temperature

Fig. 13 shows the performance of the RPR process as a function of temperature from 150°C to 650°C for conditions of duty cycle = 15%, $\text{SV} = 30,000 \text{ h}^{-1}$, and $\lambda_{\text{pulse}} = 0.76$. Fig. 13(a) displays the NO_x conversion and Fig. 13(b) shows the reductant (ethylene) conversion as a function of temperature from 150°C to 650°C for pulsing frequencies of 0.0167, 0.1, 0.333, 0.5, and 1 Hz. It can be observed that increasing the pulsing frequency from that used for a conventional LNT (e.g., 0.0167 Hz) to typical RPR values (e.g., 1 Hz) improved the NO_x conversion not only at high temperatures, but also at temperatures lower than 300°C . At temperatures higher than 450°C , the optimal pulsing frequency increased as the temperature increased. Furthermore, as shown in Fig. 13(b) the ethylene conversion improved at higher pulsing frequencies, especially at lower temperatures. Fig. 13(c) demonstrates the variation in selectivity of N_2O and NH_3 as a function of temperature at different

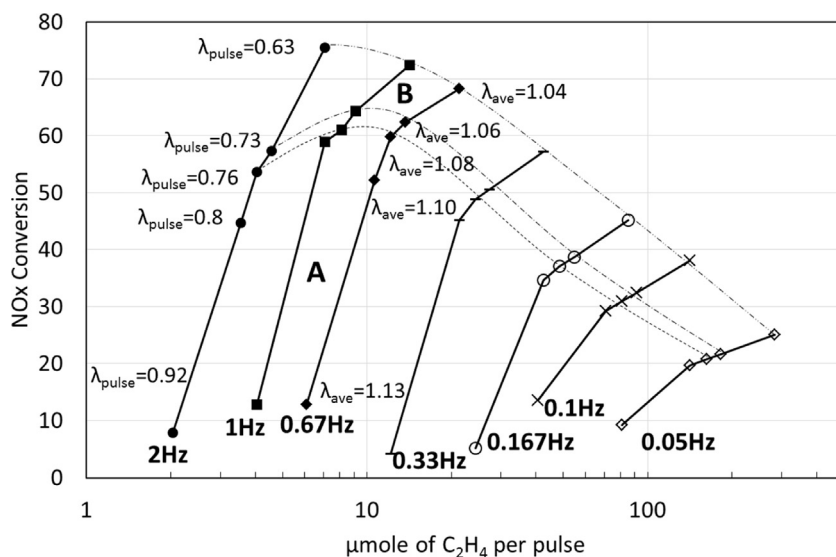


Fig. 11. The effect of pulse magnitude and pulsing frequency on NO_x conversion, plotted as a function of moles of reductant (ethylene) per pulse for 15% pulse duty cycle, inlet T = 600 °C, and SV = 30,000 h⁻¹. Solid lines show isofrequency curves and dashed lines show iso-λ_{pulse} (or isofuel penalty) lines.

pulsing frequencies. The NH₃ selectivity peaked around 450 °C and decreased at higher temperatures. The NH₃ selectivity decreased as the pulsing frequency increased over the entire temperature range. Conversely, N₂O was formed at lower temperatures, reaching maxima at 250–300 °C, and the selectivity increased as the pulsing frequency increased.

3.7. Duty cycle

All of the results presented thus far were measured with a duty cycle of 15%. The rationale for this choice was based on an early investigation into the impact of the duty cycle. The effect of duty cycle was investigated by sweeping from 5% to 30% while keeping the pulse amplitude (or λ_{pulse}) constant at 0.76. Hence, the amount of delivered reductant to the flow or the fuel penalty increased linearly with duty cycle. The tests were performed with ethylene as the reductant at 600 °C and a SV of 28,000 h⁻¹ for pulsing frequencies of f = 0.67 Hz and 0.167 Hz (P = 1.5 s and 6 s), and the results are shown in Fig. 14. One of the lines (f = 0.67 Hz) is representative of the optimal pulsing frequency at the operating conditions discussed earlier, while the other line (f = 0.167 Hz) is representative of a lower pulsing frequency with longer purges. Fig. 14 (a) shows that, with a 0.167 Hz pulsing frequency, the NO_x conversion exceeded 75% with a duty cycle of 5%, and the conversion increased only gradually at higher duty cycle values. However, with a 0.67 Hz pulsing frequency, the NO_x conversion increased dramatically beyond a duty cycle of 7.5% and achieved levels above 90% at duty cycles of 15% and above. The pulsing frequency of 0.167 Hz produced higher NO_x conversion at lower duty cycles (i.e., less fuel penalty), whereas the higher pulsing frequency of 0.167 Hz produced higher NO_x conversions at higher duty cycles (i.e., higher fuel penalty). As the duty cycle was increased, Fig. 14(b) shows that the ethylene conversion decreased due to incomplete oxidation during the increasingly longer rich pulses, and the average catalyst bed temperature increased as the duty cycle increased due to the increasing duration of the exothermic pulses.

If we consider the total amount (i.e., moles) of reductant during each pulse, the duty cycle showed similar trends as the λ_{pulse}. Specifically, whether the duty cycle increased or the pulses became richer, more moles of reductant were delivered, and the NO_x conversion initially increased rapidly and then at a reduced rate. It was desired to determine whether the effects of duty cycle and pulse

amplitude were essentially the same (i.e., two different approaches to increase the amount of reductant), or if these variables lead to other effects in the system that need to be understood. To separate the effects of duty cycle and λ_{pulse} on the NO_x conversion for a constant fuel penalty, the area under the pulse curve (e.g., area under the upstream curve in Fig. 2 which shows the amount of reductant added to the flow per pulse) was maintained at a constant fuel penalty of 5.2% while increasing the duty cycle from 5% to 50% and increasing the λ_{pulse} from 0.523 to 1.042 (i.e., decreasing the concentration of reductant). The results at 600 °C, 28,000 h⁻¹, and P = 1.5 s are shown in Fig. 15, which indicates a relatively flat area of the NO_x conversion curve (i.e., at a duty cycle ≤ 15% and λ_{pulse} < 0.83) in which the duty cycle and λ_{pulse} had similar effects on the NO_x conversion; i.e., a short, but very rich pulse produced the same NO_x conversion as a longer but less rich pulse for a given fuel penalty. Therefore, the performance of RPR over this region is only dependent on the integrated amount of reductant available in the flow. However, outside of this region, the NO_x conversion dropped significantly as the duty cycle continued to increase and the λ_{pulse} continued to decrease while maintaining the same fuel penalty. As indicated in Fig. 11, the rich lambda must be below a certain rich level (e.g., λ_{pulse} < 0.80 to 0.85) in order to obtain high NO_x conversion. As the duty cycle increased beyond 15% and the rich magnitude decreased to maintain the same fuel penalty, the rich lambda did not achieve this minimum level, and the NO_x conversion began to decrease. Similar observations have been reported previously on conventional LNTs. At low temperatures where the release and reduction of the NO_x is kinetically limiting, a longer/low concentration reductant pulse enhances the overall NO_x conversion. Conversely, at T > 450 °C (the case of RPR), these reactions occur very rapidly; therefore, high concentration/shorter reductant pulses result in more effective purging of the LNT, enhancing the overall NO_x conversion [22].

4. Discussion

4.1. The optimal frequency for NO_x conversion with RPR

The NO_x conversion of a LNT during RPR operation was assessed as a function of catalyst type, NO_x storage capacity, temperature, space velocity, NO_x concentration, pulsing frequency, amplitude, and duty cycle. The bed temperatures and the concentrations of

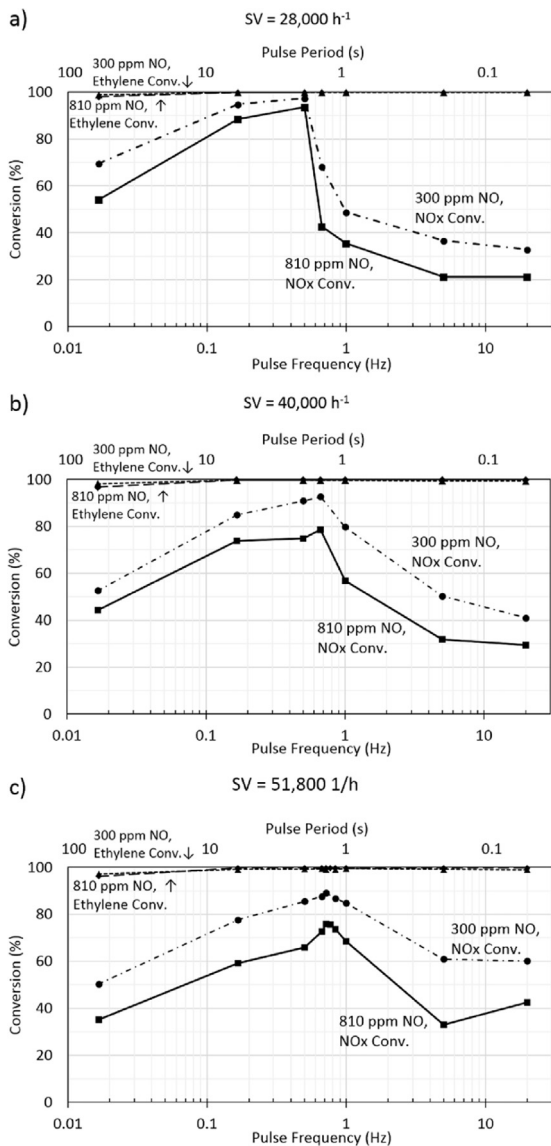


Fig. 12. Comparison of frequency sweep results for feed NO of 300 ppm and 810 ppm at (a) $SV = 28,000 \text{ h}^{-1}$, (b) $SV = 40,000 \text{ h}^{-1}$, and (c) $SV = 51,800 \text{ 1/h}$, 15% duty cycle, $\lambda_{\text{pulse}} = 0.83$, and inlet $T = 600^\circ\text{C}$.

NO_x, ethylene, and reaction products emitted from the reactor were measured for the first time as the pulsing frequency was varied from $f = 1/60 \text{ Hz}$ to 20 Hz , (i.e., over more than three orders of magnitude). These results clearly demonstrated that, for a given set of operating conditions, there was an optimal pulsing frequency that achieved the highest NO_x conversion for a constant fuel penalty. This peak NO_x conversion occurred in the range of 0.5 Hz to 1 Hz with ethylene as the reductant. Both the peak conversion value and the optimal frequency depended on the operating conditions (e.g., flow velocity, reductant concentration, and temperature). However, we found that the feedgas NO_x concentration did not affect the optimal frequency, although the conversion levels depended on the NO_x concentration.

For the temperature range of $450\text{--}600^\circ\text{C}$, the overall frequency response of the RPR process can be divided into two regimes: low frequencies (i.e., frequencies lower than the optimal frequency) and high frequencies (i.e., frequencies higher than the optimal frequency). The existence of an optimal frequency can be explained as a trade-off between NO_x storage efficiency and NO_x reduction effectiveness in the low and high frequency regimes as follows;

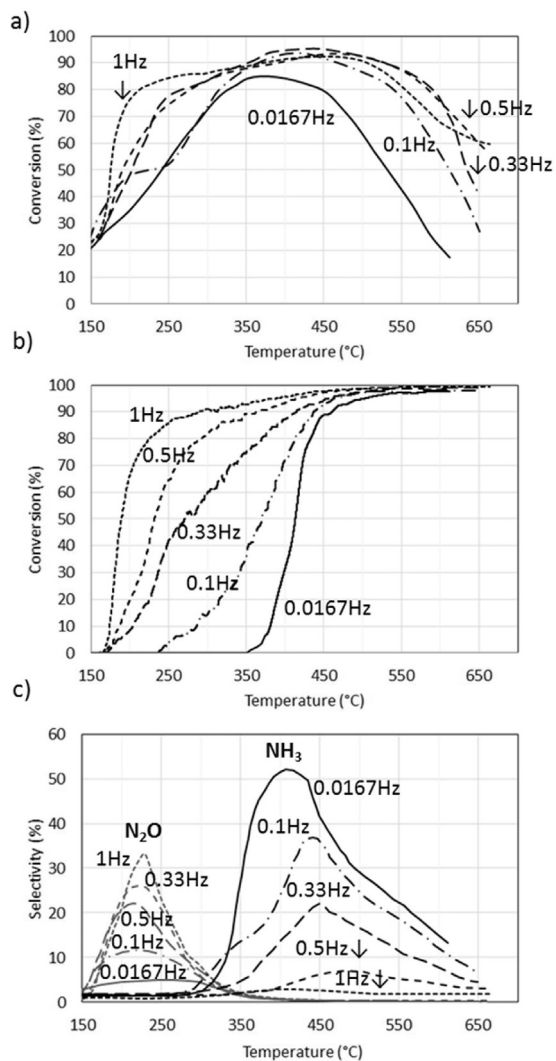


Fig. 13. Temperature sweep results for different pulsing frequencies $f = 0.0167, 0.1, 0.33, 0.5$, and 1 Hz for ethylene at 15% duty cycle, $\lambda_{\text{pulse}} = 0.76$, and $SV = 30,000 \text{ h}^{-1}$ (a) NO_x conversion (b) ethylene conversion (c) NH₃ and N₂O selectivity.

(1) By decreasing the frequency relative to the optimal frequency, the NO_x reduction and purging of the LNT becomes very complete; however, the lean period becomes longer, resulting in lower NO_x storage efficiency and lower overall cycle-averaged NO_x conversion. (2) By increasing the frequency relative to the optimal frequency, the storage becomes more efficient due to shorter lean periods, but the effectiveness of the rich pulses for converting the stored NO_x and purging the LNT decreases. This is mainly due to axial mixing of the rich pulse which results in less capability to produce a sufficiently rich mixture at any point to effectively react with and remove the stored NO_x.

4.1.1. NO_x reduction: governing factor in the high frequency regime

The decreasing effectiveness of the rich period for purging the LNT as the frequency increased was partly due to axial mixing of the reductants. While the mixer and injection system were designed to minimize axial convective mass transfer [10], some axial mixing was unavoidable due to turbulent motion at the mixer, molecular diffusion, and viscous wall shear. The shape of the reductant pulse as a function of pulsing frequency is shown in Fig. 9, which indicates that as the pulsing frequency increased, more mixing occurred between the reductant pulses and the main flow. Fig. 16

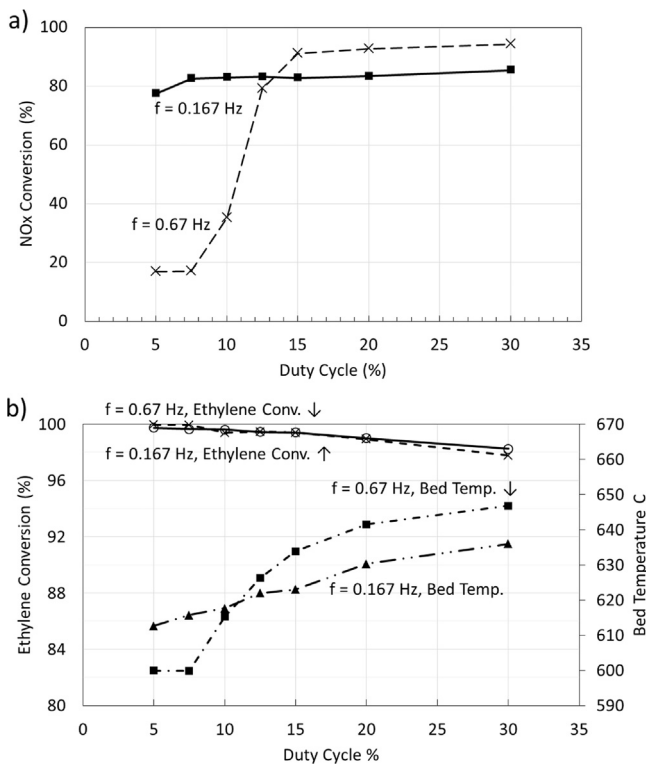


Fig. 14. Representative duty cycle sweeps for $f = 0.67$ and 0.167 ($P = 1.5 \text{ s}$ and $P = 6 \text{ s}$) for inlet $T = 600^\circ\text{C}$, $\lambda_{\text{pulse}} = 0.76$, and $\text{SV} = 28,000 \text{ h}^{-1}$. (a) NO_x conversion (b) ethylene conversion and catalyst bed temperature.

illustrates this pulse mixing process. As the pulse moves downstream, the leading and trailing edges of each pulse mix with the adjacent lean zones. As a result, the maximum reductant concentration drops below the intended concentration. In Fig. 16, the grey zones indicate an overall lean mixture where some of the reductant diffuses in both directions, but the concentration is below the level required to achieve stoichiometry (indicated by the dashed blue lines). The black zones indicate a rich mixture where the reductant concentration exceeds the level required to achieve stoichiometry. The red line is the reductant concentration arriving at the front of the LNT during the pulse. Even with the forward and backward diffusion of some of the reductant, Fig. 16(a) shows that, with sufficiently long pulses, the reductant concentration at the front face of the LNT exceeds the stoichiometric level and thereby generates a rich mixture for a significant period of time, resulting in good purging of the LNT. However, Fig. 16(b) shows that, with shorter pulses (i.e., higher frequencies), a higher percentage of the pulse diffuses in both directions into the lean zones, resulting in inadequate purging of the LNT. These mixed zones produce more complete oxidation of the HC, leaving less and less of the “rich” zone, resulting in decreasing CO, C₂H₄, and NH₃ and increasing CO₂, as seen in Figs. 6–8. Fig. 16(c) shows that, with sufficiently short pulses, essentially all of the reductant mixes with the lean exhaust, and the LNT is not purged at all.

4.1.2. NO_x storage: governing factor in the low frequency regime

To qualitatively illustrate how the NO_x storage and removal vary in RPR between a low frequency and a high frequency, Fig. 17 illustrates the coverage of NO_x storage sites as a function of time at two pulsing frequencies of 0.0167 Hz and 0.1 Hz (i.e., $P = 60 \text{ s}$ and 10 s). Fig. 17 (a) illustrates a single storage and reduction cycle at $P = 60 \text{ s}$. Here, the storage and removal periods are long, such that complete NO_x storage and purging are achieved. However, the maximum storage capacity is reached before the end of the lean storage period

and for a portion of this period the storage rate is negligible. The slope of the black dashed line connecting the end points is proportional to the mean storage rate, and thus to storage efficiency. These qualitative curves are guided by other transient measurements with a mass spectrometer and a FTIR with moderate time resolution that provide the general shape of the time dependent storage and removal of NO_x from the catalyst.

Fig. 17(b) illustrates storage and reduction cycles at a higher frequency ($P = 10 \text{ s}$). Here, the lean storage period is short enough that the NO_x storage sites are never completely filled. Furthermore, as argued in the discussion of Fig. 16, the pulses become axially mixed as the frequency increases, resulting in inadequate reduction of the stored NO_x. Therefore, the purging does not proceed to completion. As a result, the storage curve begins at a value greater than zero. In spite of the storage limitations imposed by the fast pulsing frequency, the mean storage rate is greater than in the low frequency case, indicating the potential for higher NO_x conversion at higher frequencies.

4.2. Dependence of the optimal frequency on operating conditions

It was observed in Fig. 13 (a) that the optimum pulsing frequency increased with increasing temperature at $T > 450^\circ\text{C}$. This is attributed to the fact that the NO_x storage capacity of the LNT decreased at higher temperatures, which imposed a need to increase the frequency in order to shorten the lean period and maintain high NO_x storage efficiency.

The dependence of the optimal frequency on space velocity can also be explained by the limited NO_x storage capacity of the LNT. At higher flow rates, there was a higher flux of NO_x, so the maximum amount of NO_x stored at the lower space velocity would be achieved in a shorter time at the higher space velocity. Therefore, to obtain high NO_x storage efficiencies at the higher flow rates, the duration of the lean period needed to be decreased. Consistent with this premise, the optimal frequencies at 28,000 and 40,000 h^{-1} (i.e., 0.50 and 0.67 Hz) were approximately proportional to the space velocities.

The insensitivity of the optimum frequency to NO_x concentration can be explained using the Langmuir adsorption isotherms [23]. The NO_x storage rate is proportional to the gas phase NO_x concentration for low levels of NO_x storage, which occur as a result of the very short lean storage period with RPR. Therefore, as the gas phase concentration of NO_x was increased, the rate of NO_x storage was increased proportionally, and the optimal frequency remained the same.

4.3. NO_x conversion vs. fuel penalty

Considering the results of Fig. 11(a), the NO_x conversion increased when increasing the concentration of injected reductant (i.e., decreasing the λ_{pulse}) at a constant frequency. The rate of improvement in conversion was high for lower amounts (i.e., moles) of reductant (i.e., λ_{pulse} between 0.92 to ca. 0.80), but the rate of improvement was significantly reduced for higher amounts of reductant (i.e., λ_{pulse} richer than 0.80). This saturating trend may be due to the low order of the reaction with respect to ethylene partial pressure [24,25]. Therefore, at any given temperature and pulsing frequency, the λ_{pulse} should be selected near the point of saturation at the highest slope on the isofrequency curves to ensure maximum NO_x conversion with minimal fuel penalty.

A drawback of the richer λ_{pulse} is that it would increase the fuel economy penalty for a constant frequency. However, the richer pulses allow the frequency to be increased while maintaining the same moles of reductant, and the shorter lean period would increase the average NO_x storage efficiency and therefore the overall NO_x conversion while maintaining the same fuel economy

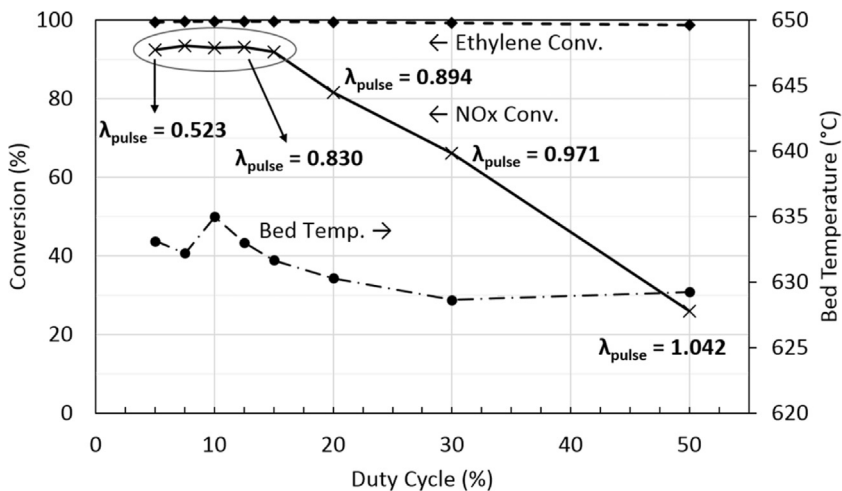


Fig. 15. Pulse amplitude/duty cycle sweep for constant 5.2% fuel economy penalty. $f = 0.67 \text{ Hz}$, $SV = 28,000 \text{ h}^{-1}$, and inlet $T = 600^\circ\text{C}$ showing NOx and ethylene conversions and catalyst bed temperature.

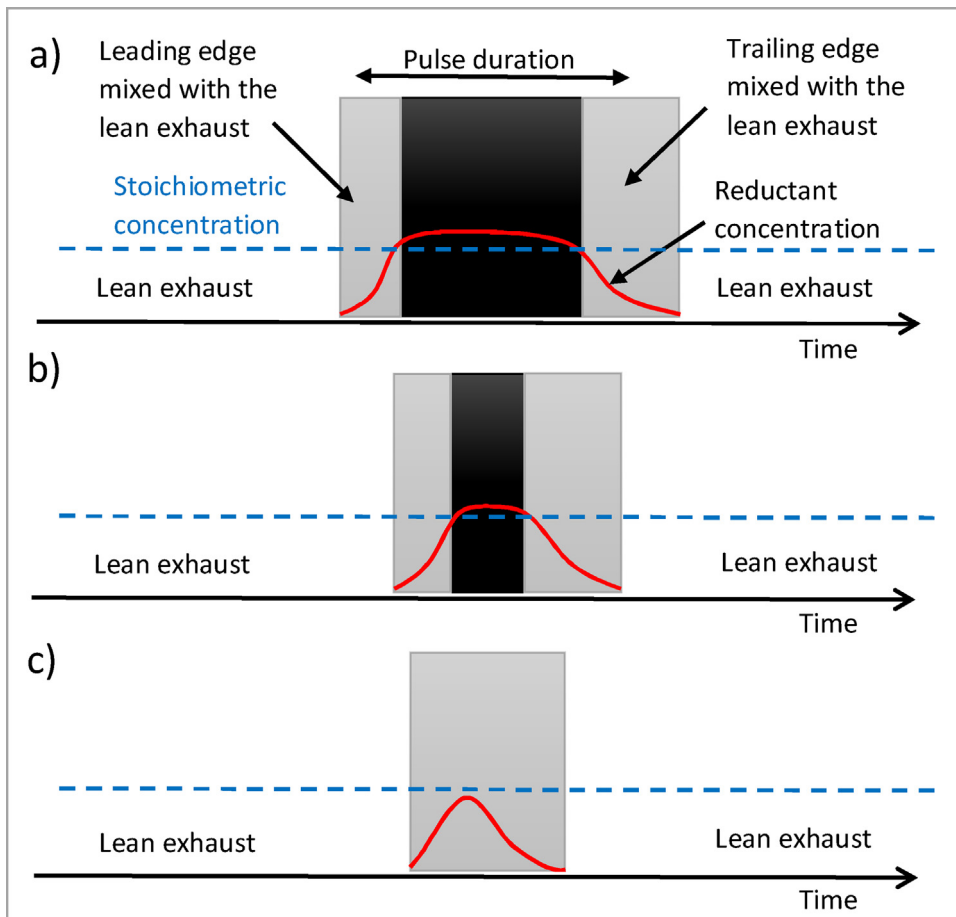


Fig. 16. Schematics of temporal distribution of reductants at catalyst inlet as a pulse enters the catalyst for different pulsing frequencies where $f_a < f_b < f_c$. Gray zones indicate overall lean mixtures during a pulse, while black zones indicate a rich mixture. The red line is the reductant concentration during the pulse. The blue dashed line shows the stoichiometric concentration. (For interpretation of the references to colour in this figure legend, the reader is referred to the web version of this article.)

penalty. This fuel economy analysis neglects any losses during the lean to rich transitions and the rich to lean transitions.

Fig. 14(a) showed that, with a λ_{pulse} of 0.76 and a space velocity of $28,000 \text{ h}^{-1}$, a 5% duty cycle provided maximum NOx conversion with a 0.167 Hz pulsing frequency (i.e., 0.3 s rich pulses), but a duty cycle of 15% was needed to provide maximum NOx conversion with a 0.67 Hz pulsing frequency (i.e., 0.225 s rich pulses). For both fre-

quencies, the improvement in NOx conversion was only marginal as the duty cycle (and the fuel penalty) continued to increase. These pulse durations correspond to a minimum number of moles of reductant. This suggested that the proper combination of frequency, duty cycle, and λ_{pulse} needed to be selected to provide the minimum number of moles of reductant during the hydrocarbon pulses to purge the LNT. However, further increases in the duty

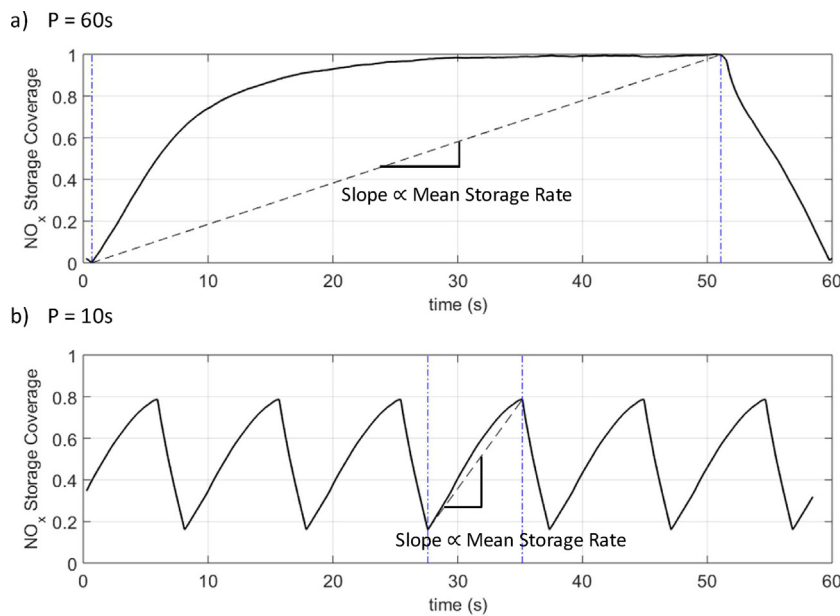


Fig. 17. Coverage of NO_x storage sites during storage and reduction at pulsing frequencies of (a) 0.0167 Hz and (b) 0.1 Hz. The slope of the black dashed line is proportional to the mean NO_x storage rate over the storage period.

cycle would only increase the fuel penalty while providing only incremental improvements in the NO_x conversion for a constant frequency and λ_{pulse} .

Fig. 14 showed that increasing the duty cycle while holding the moles of reductant (i.e., fuel penalty) constant by increasing the λ_{pulse} (i.e., reducing the concentration of reductants) provided essentially constant NO_x conversion as long as the λ_{pulse} achieved a minimum level of ca. 0.85. However, a λ_{pulse} greater than 0.85 did not purge the LNT adequately, even when the pulse duration was increased to provide the same moles of reductant. The data with a pulsing frequency of 0.67 Hz in Figs. 14(a) and Fig. 15 together suggest that a minimum number of moles of reductant at a concentration required to achieve a λ_{pulse} of 0.85 or lower are needed to adequately purge the LNT and achieve high NO_x conversions.

As long as the combination of duty cycle, frequency, and λ_{pulse} (referred to here as the “base case”) provided the minimum number of moles of reductant at the necessary concentration to purge the LNT, increasing the duty cycle would in theory allow the frequency to be increased proportionately (again neglecting any losses in fuel economy due to the lean/rich and rich/lean transitions). The shorter lean period would increase the NO_x conversion, while the duration of the rich period with the higher duty cycle and the higher frequency would remain the same as the base case. However, the fuel economy penalty would increase due to the higher proportion of time in the rich condition with the higher duty cycle. To reduce the fuel economy penalty to the base case, the magnitude of the λ_{pulse} would also need to be decreased proportionately. As long as the resulting λ_{pulse} remained below 0.85, the NO_x conversion would stay high and theoretically the fuel penalty would be similar to the base case. The requirement to maintain the λ_{pulse} at 0.85 or below limits the range of duty cycles that can be considered.

To summarize, any change in the operating conditions that decreased the effective NO_x storage capacity of the LNT (such as increasing the temperature) increased the optimal pulsing frequency. Also, any change in the operating conditions that increased the demanded amount of NO_x storage capacity (such as increasing the SV) increased the optimal pulsing frequency. The exception to this last observation was the increase in feedgas NO_x concentration, where the higher storage rate with the higher NO_x concentra-

tion maintained the optimal pulsing frequency at the same level as at the lower NO_x concentration. Finally, decreasing the λ_{pulse} enhanced the effectiveness of the reduction step and increased the optimal frequency. The shorter rich period would minimize the fuel economy penalty with the richer λ_{pulse} while still purging the LNT adequately, and the shorter lean period would increase the NO_x conversion. Increasing the duty cycle would also increase the optimal frequency, but the magnitude of the λ_{pulse} would need to be reduced to minimize the fuel economy penalty. As long as the λ_{pulse} remained at 0.85 or below, the NO_x conversion would remain high.

4.4. Reaction products

As the frequency was increased from conventional LNT operation (i.e., $f = 1/60$ Hz), the cycle-averaged CO concentration decreased significantly to around zero at the optimal frequency. Also, the ethylene conversion increased as the frequency was increased from $f = 1/60$ Hz to the optimal frequency ($f = 0.5$ Hz). These observations can be explained by partial mixing of the rich pulse with the leading and trailing lean gas flows.

The time-averaged bed temperature increased as the pulsing frequency was increased from the conventional LNT frequency to the optimal RPR frequency. This was consistent with more complete oxidation of C₂H₄ to CO₂ and H₂O due to the increased axial mixing observed with increasing frequency in Fig. 9, which resulted in a larger exotherm than the partial oxidation of the C₂H₄ to CO (and presumably H₂) at lower frequencies. Furthermore, the reduction of NO_x is exothermic, so the increasing NO_x conversion below the optimum frequency also contributed slightly to the increased exotherm. Above the optimum frequency, the NO_x conversion dropped, which may account for the small drop in the measured temperature even though the exotherm from complete C₂H₄ oxidation to CO₂ and H₂O should have remained fairly constant.

N₂O selectivity reached a maximum at around 250 °C and increased as the frequency increased. This observation may be explained by previous studies of N₂O and N₂ formation over Pt/Ba/Al₂O₃ LNT catalysts using isotopically labeled NO feed [26–29]. Most of the studies relate N₂O formation to the coexis-

tence of dissociated and non-dissociated NO in this temperature range (around 250 °C), where N₂O can be formed over reduced Pt or Rh catalysts by the reaction of NO_{ads} with N_{ads} [27,30]. The rate of reduction of these sites is considered fast at 250 °C; hence, there is often a primary peak in N₂ and N₂O concentration immediately after a transition from lean to rich conditions [16,28,30–32]. Therefore, it can be concluded that at higher pulsing frequencies, the number of lean to rich transitions per unit time increased which increased the selectivity to N₂O.

On the other hand, NH₃ appeared at the outlet of the catalyst with a slight delay after a lean to rich transition, and longer/richer pulses were favorable for formation of NH₃ [22,33,34]. The delay in NH₃ appearance was attributed to the oxidation, decomposition, or further reaction of NH₃ with surface species as it traveled downstream of the catalyst [22,35,36]. This delay explained the drop in NH₃ concentration at the higher pulsing frequencies of RPR. For instance, at the optimal pulsing frequencies tested here, the rich pulse duration (0.15 s to 0.3 s) was shorter than the time required for appearance of NH₃ at the outlet of the catalyst. In addition, due to axial mixing at higher frequencies, the pulse was on average less rich, which also may have reduced the selectivity to ammonia.

5. Conclusions

The use of rapidly pulsed reductants on a conventional LNT catalyst sample was studied experimentally using a synthetic flow reactor and a high frequency injection system. The effects of the pulsing frequency, amplitude, duty cycle, temperature, space velocity, and NO_x concentration on the NO_x conversion and the reaction products were investigated. The following conclusions were found for the temperature range of 450–600 °C:

- NO_x storage capability was required in the catalyst for RPR to work.
- Useful NO_x conversion was obtained only when the hydrocarbon pulses were net rich, even though the overall cycle-averaged flow was lean.
- There existed an optimal pulsing frequency for NO_x conversion on the order of 0.5–1 Hz with RPR.
- In the range of operating temperature considered in this study, 450–600 °C, the pulsing frequency could be divided into a low frequency regime (lower than the optimal frequency) and a high frequency regime (higher than the optimal frequency). By decreasing the frequency relative to the optimal frequency, the NO_x storage efficiency decreased due to a decrease in the average NO_x storage efficiency during the increasingly longer lean periods. By increasing the frequency relative to the optimal frequency, the NO_x conversion dropped due to incomplete purging during the rich periods.
- The rich lambda needed to be below 0.85 to achieve the maximum NO_x conversion for the set of conditions in this study.
- The optimal pulsing frequency was a function of space velocity, temperature, and reductant dosing during the pulses and increased as any of these parameters were increased.
- As the feedgas NO_x concentration was increased, both the NO_x and reductant (ethylene) conversion decreased, but the optimal frequency remained unchanged due to higher storage rates with the higher NO_x concentration.
- By increasing the amount of reductant injected (either by increasing the pulse amplitude or the duty cycle), the NO_x conversion increased with an asymptotic approach to saturation. Generally, the optimal pulsing frequency increased as more reductant was injected.
- As the pulsing frequency was increased, the N₂O selectivity increased and NH₃ selectivity decreased.

- A map of pulsing frequency, amplitude (λ_{pulse}), and duty cycle could be used to obtain the maximum NO_x conversion with the lowest fuel economy penalty for various operating conditions. If implemented on a vehicle, such a map could be used with control algorithms to maximize the NO_x conversion and minimize the fuel penalty with RPR.

Acknowledgments

The University of Michigan authors acknowledge support from Ford Motor Company within the UM–Ford Alliance Program to carry out this work. We would also like to thank Brent Patterson, Benjamin Corson, and Jun Lin Tan for help with the measurements. Evgeny Smirnov, Dirk Roemer, and Brendan Carberry of Ford Motor Co. also gave thoughtful comments on this work.

References

- [1] D. Stanton, S. Charlton, P. Vajapeyazula, Diesel Engine Technologies Enabling Powertrain Optimization to Meet US Greenhouse Gas Emissions, SAE Technical Paper, 2013.
- [2] J.B. Heywood, Internal Combustion Engine Fundamentals, McGraw-Hill, New York, 1988.
- [3] T. Johnson, Vehicular emissions in review, *SAE Int. J. Engines* 7 (2014) 1207–1227.
- [4] T.V. Johnson, Diesel emission control in review, in: US Dept. of Energy Diesel Engine Efficiency and Emissions Reduction (DEER) Conference, Detroit, 2006.
- [5] L. Yang, V. Franco, A. Campestrini, J. German, P. Mock, NO_x Control Technologies for Euro 6 Diesel Passenger Cars, ICCT White Paper, 2015 (Accessed on Apr., 2016) Search PubMed.
- [6] Y. Li, S. Roth, J. Detting, T. Beutel, Effects of lean/rich timing and nature of reductant on the performance of a NO_x trap catalyst, *Top. Catal.* 16 (2001) 139–144.
- [7] C. Dujardin, A. Kouakou, F. Fresnet, P. Granger, Reaction pathways for ammonia formation on lean NO_x Trap/Reduction system: a spectroscopic infrared investigation, *Top. Catal.* 56 (2013) 151–156.
- [8] R.S. Larson, J.A. Pihl, V.K. Chakravarthy, T.J. Toops, C.S. Daw, Microkinetic modeling of lean NO_x trap chemistry under reducing conditions, *Catal. Today* 136 (2008) 104–120.
- [9] R.D. Clayton, M.P. Harold, V. Balakotaiah, Performance features of Pt/BaO lean NO_x trap with hydrogen as reductant, *AIChE J.* 55 (2009) 687–700.
- [10] A. Reihani, B. Corson, J.W. Hoard, G.B. Fisher, E. Smirnov, D. Roemer, J. Theis, C. Lambert, Rapidly pulsed reductants in diesel NO_x reduction by lean NO_x traps: Effects of mixing uniformity and reductant type, *SAE Int. J. Engines* 9 (2016).
- [11] T. Lesage, C. Verrier, P. Bazin, J. Saussey, S. Malo, C. Hedouin, G. Blanchard, M. Daturi, Comparison between a Pt–Rh/Ba/Al₂O₃ and a newly formulated NO_x-trap catalysts under alternate lean-rich flows, *Top. Catal.* 30 (2004) 31–36.
- [12] C.C. Perng, V.G. Easterling, M.P. Harold, Fast lean-rich cycling for enhanced NO_x conversion on storage and reduction catalysts, *Catal. Today* 231 (2014) 125–134.
- [13] C. Lambert, R. Hammerle, R. McGill, M. Khair, C. Sharp, Technical advantages of urea SCR for light-duty and heavy-duty diesel vehicle applications, *SAE Trans.* 113 (2004) 580–589.
- [14] T.V. Johnson, Diesel Emission Control in Review, 2008 SAE World Congress, SAE Technical Paper, 2008 (pp. 0069).
- [15] J. Theis, J. Ura, C. Goralski, H. Jen, E. Thanasiu, Y. Graves, A. Takami, H. Yamada, S. Miyoshi, The Effect of Ceria Content on the Performance of a NO_x Trap, SAE Technical Paper, 2003.
- [16] Y. Ji, J.-S. Choi, T.J. Toops, M. Crocker, M. Naseri, Influence of ceria on the NO_x storage/reduction behavior of lean NO_x trap catalysts, *Catal. Today* 136 (2008) 146–155.
- [17] Y. Bisaiji, K. Yoshida, M. Inoue, K. Umamoto, T. Fukuma, Development of Di-Air–A new diesel deNO_x system by adsorbed intermediate reductants, *SAE Int. J. Fuels Lubr.* 5 (2011) 380–388.
- [18] M. Inoue, Y. Bisaiji, K. Yoshida, N. Takagi, T. Fukuma, deNO_x performance and reaction mechanism of the Di-Air system, *Top. Catal.* 56 (2013) 3–6.
- [19] Y. Bisaiji, K. Yoshida, M. Inoue, N. Takagi, T. Fukuma, Reaction mechanism analysis of Di-Air–Contributions of hydrocarbons and intermediates, *SAE Int. J. Fuels Lubr.* 5 (2012) 1310–1316.
- [20] S. Cavallaro, Ethanol steam reforming on Rh/Al₂O₃ catalysts, *Energy & Fuels* 14 (2000) 1195–1199.
- [21] C. Resini, L. Arrighi, M.C.H. Delgado, M.A.L. Vargas, L.J. Alemany, P. Riani, S. Berardinelli, R. Marazza, G. Busca, Production of hydrogen by steam reforming of C₃ organics over Pd–Cu/γ-Al₂O₃ catalyst, *Int. J. Hydrogen Energy* 31 (2006) 13–19.
- [22] C.D. DiGiulio, J.A. Pihl, J.-S. Choi, J.E. Parks, M.J. Lance, T.J. Toops, M.D. Amiridis, NH₃ formation over a lean NO_x trap (LNT) system: effects of lean/rich cycle timing and temperature, *Appl. Catal. B: Environ.* 147 (2014) 698–710.

- [23] H.S. Fogler, *Essentials of Chemical Reaction Engineering*, Pearson Education, 2010.
- [24] R. Burch, J. Breen, F. Meunier, A review of the selective reduction of NO_x with hydrocarbons under lean-burn conditions with non-zeolitic oxide and platinum group metal catalysts, *Appl. Catal. B: Environ.* 39 (2002) 283–303.
- [25] H. Nguyen, M.P. Harold, D. Luss, Spatiotemporal behavior of Pt/Rh/CeO₂/BaO catalyst during lean-rich cycling, *Chem. Eng. J.* 262 (2015) 464–477.
- [26] L. Lietti, N. Artioli, L. Righini, L. Castoldi, P. Forzatti, Pathways for N₂ and N₂O formation during the reduction of NO_x over Pt–Ba/Al₂O₃ LNT catalysts investigated by labeling isotopic experiments, *Ind. Eng. Chem. Res.* 51 (2012) 7597–7605.
- [27] L. Lietti, L. Righini, L. Castoldi, N. Artioli, P. Forzatti, Labeled ¹⁵NO study on N₂ and N₂O formation over Pt–Ba/Al₂O₃ NSR catalysts, *Top. Catal.* 56 (2013) 7–13.
- [28] J. Breen, R. Burch, C. Fontaine-Gautrelet, C. Hardacre, C. Rioche, Insight into the key aspects of the regeneration process in the NO_x storage reduction (NSR) reaction probed using fast transient kinetics coupled with isotopically labelled ¹⁵NO over Pt and Rh-containing Ba/Al₂O₃ catalysts, *Appl. Catal. B: Environ.* 81 (2008) 150–159.
- [29] H. Wang, R. Tobin, C.L. DiMaggio, G.B. Fisher, D.K. Lambert, Reactions of N and NO on Pt (335), *J. Chem. Phys.* 107 (1997) 9569–9576.
- [30] D. Mráček, P. Kočí, M. Marek, J.-S. Choi, J.A. Pihl, W.P. Partridge, Dynamics of N₂ and N₂O peaks during and after the regeneration of lean NO_x trap, *Appl. Catal. B: Environ.* 166 (2015) 509–517.
- [31] W.S. Epling, A. Yezerski, N.W. Currier, The effects of regeneration conditions on NO_x and NH₃ release from NO_x storage/reduction catalysts, *Appl. Catal. B: Environ.* 74 (2007) 117–129.
- [32] R.G. Tonkyn, R.S. Disselkamp, C. Peden, Nitrogen release from a NO_x storage and reduction catalyst, *Catal. Today* 114 (2006) 94–101.
- [33] J.A. Pihl, J.E. Parks, C.S. Daw, T.W. Root, Product Selectivity During Regeneration of Lean NO_x Trap Catalysts, SAE Technical Paper, 2006.
- [34] J. Wang, Y. Ji, V. Easterling, M. Crocker, M. Dearth, R.W. McCabe, The effect of regeneration conditions on the selectivity of NO_x reduction in a fully formulated lean NO_x trap catalyst, *Catal. Today* 175 (2011) 83–92.
- [35] L. Cumaranatunge, S. Mulla, A. Yezerski, N. Currier, W. Delgass, F. Ribeiro, Ammonia is a hydrogen carrier in the regeneration of Pt/BaO/Al₂O₃ NO_x traps with H₂, *J. Catal.* 246 (2007) 29–34.
- [36] B. Pereda-Ayo, J.R. González-Velasco, R. Burch, C. Hardacre, S. Chansai, Regeneration mechanism of a Lean NO_x Trap (LNT) catalyst in the presence of NO investigated using isotope labelling techniques, *J. Catal.* 285 (2012) 177–186.